Equalization for Intracortical Microstimulation Artifact Reduction

Philip Chu

Electrical Engineering and Computer Sciences
University of California at Berkeley

Technical Report No. UCB/EECS-2013-76
http://www.eecs.berkeley.edu/Pubs/TechRpts/2013/EECS-2013-76.html

May 16, 2013

Equalization for Intracortical Microstimulation Artifact Reduction

Philip Chu

Department of Electrical Engineering, University of California at Berkeley

Abstract: I present a method for decreasing the duration of artifacts present during intra-cortical microstimulation (ICMS) recordings by using techniques developed for digital communications. I use a Zero-Forcing Equalizer (ZFE) to shape a stimulus pattern with the aim of reducing artifact length. The results find that using the ZFE stimulus has the potential to reduce artifact duration by more than 70%. Continuing work and current considerations for the hardware implementation of the equalizer are presented.

Keywords: Microstimulation, ICMS, Artifact, Neural Recordings, LFP, ZFE, Equalization, Linearity

Introduction

Recent advancements in neural stimulation have given hope to patients of spinal cord injuries, Parkinson's Disease and numerous other debilitating neurological conditions. A key tool in these advancements has been Intracortical Microstimulation (ICMS), a technique for exciting responses in neuron groups using electrical current. The practice involves stimulating and recording implants in the brain for the application of the current pulses and subsequent response measurement. In addition to therapeutic and reconstructive applications, ICMS can be used to illuminate the brain's organization [1-2].

The ability to accurately record neural signals from both high-frequency Action Potentials (AP) and low-frequency Local Field Potentials (LFP) before and after stimulation is desirable for neuroscientists and engineers alike [2-3]. In neural implants, this capability enables true bi-directional communication between the device and the brain. A major hurdle to the simultaneous stimulation and recording of brain activity is the artifact that occurs immediately after stimulation [2]. This artifact, exemplified in Figure 1, saturates recording equipment and distorts microstimulation recordings, rendering milliseconds of recording data useless. Our primary goal is to prevent the artifacts in the LFP recordings and thereby reduce the "dead time"—this refractory period between stimulation and recordable data.

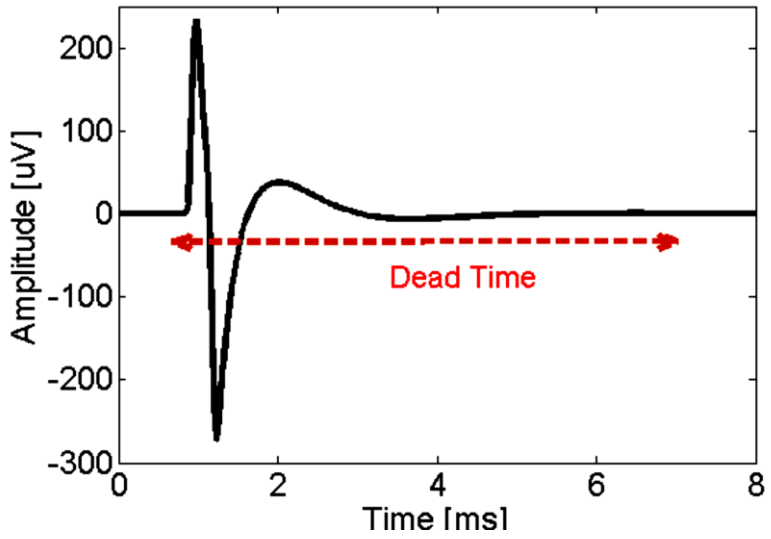

Figure 1: An LFP Artifact Resulting from 40μA Current Stimulus

Notice that while the artifact is Figure 1 has a peak amplitude of 200μV, artifacts can have peak amplitudes of hundreds of millivolts depending on location and stimulation strength. Since neural signals have amplitudes on the order of 10μV, this artifact completely drowns out neural signal. "Dead time" will be strictly defined in the Artifact Estimation section.

Reducing the duration of the artifact has the promise to improve crucial aspects of ICMS. Most directly, it could uncover neural activity occurring immediately after stimulation. Additionally, it could enable higher frequency stimulation and also improve the practices such as recording-triggered ICMS described in [3]. The presented technique aims to prevent the artifact from occurring through the design of the current stimulus waveform. Once the artifact is well-characterized, a linear equalizer is applied to reduce dead time.

The Zero-Forcing Equalizer is a linear equalizer that reduces the time-domain smearing of a pulse caused by the low-pass nature of a channel. Taking in a time-domain channel response and desired output, a ZFE produces an input sequence that will result in a channel

output near our desired output. The full algorithm will be discussed in detail in the Linear Equalization section.

Literature Review

Many published techniques aim to cope with the effects of the artifact as opposed to reduce the artifact itself. In [5], the authors mitigate the effects by disconnecting the input stage while the artifact is occurring. This prevents the input amplifiers from saturating and improves the hardware performance. In [6], artifacts are by characterizing the artifact and then subtracting it from the overall recording. While this approach removes the artifact from the recordings, the hardware considerations involved with recording the high amplitude artifact are not ameliorated. In [7], the practice of Deep Brain Stimulation (DBS) uses a fixed frequency stimulus pattern. A notch filter is placed before the recording equipment to attempt to filter out the artifact. Lastly in [8], frequency and electrode positioning are used to mitigate the artifact. While these techniques may be effective in coping with the effects of the artifact, our proposed methodology attempts to directly reduce the artifact width. To do so, research into the hardware and stimulation protocols of ICMS is necessary.

Background

The ICMS experiments described in this report were done in the Carmena Lab at UC Berkeley together with Aaron Koralek. The setup for these experiments is shown in Figure 2. All experiments were done in accordance with the Animal Care and Use Committee at the University of California, Berkeley.

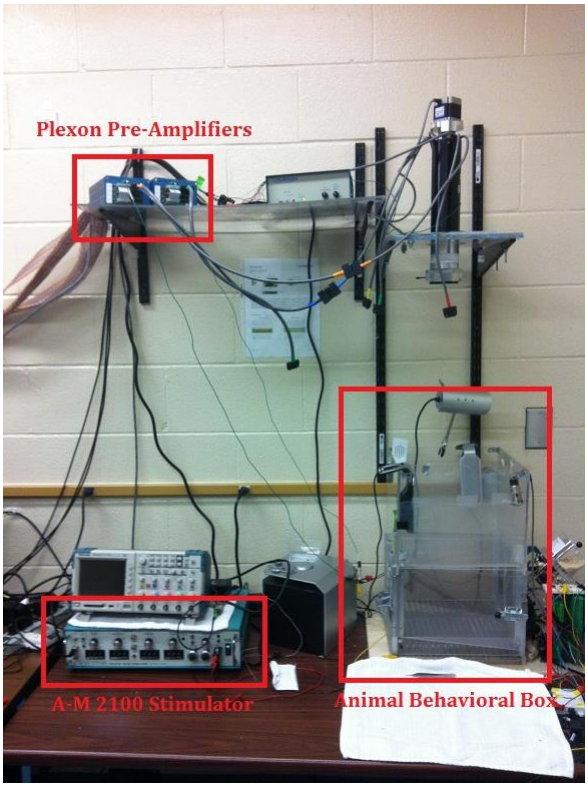

Figure 2: Typical ICMS Setup

An AM-2100 Isolated Pulse Stimulator generates a current pulse that is sent into the high-impedance stimulating electrode implant. Typical current amplitudes are in the 10-100's μA range [1]. In our experiments, we are stimulating the primary motor cortex (M1) and recording from the dorsolateral striatum (DLS) of a rat, as shown in Figure 3. The rat is awake and free-moving but tethered by the wired stimulator. The current stimulation evokes an electrical response in the brain, which we want to record.

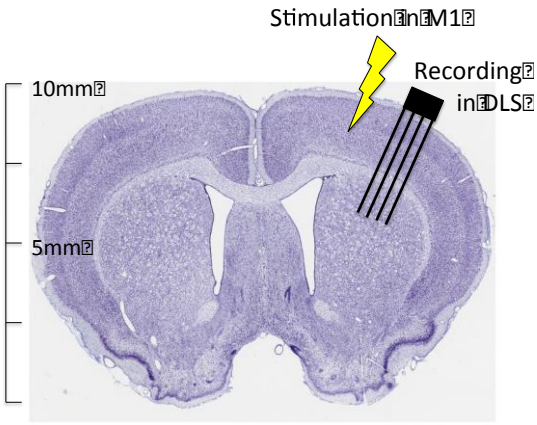

Figure 3: Stimulation and Recording Electrode Placement

The recording system begins with an array of 16 tungsten recording electrodes, which feeds the neural voltage signal into an acquisition system. We use the Plexon Multi-Channel Acquisition Processor (MAP), which consists of several gain stages and filters. After this conditioning, the signal is sampled at 40kHz and quantized, and the high-frequency spikes and lower frequency LFP recordings are sorted using the accompanying Plexon software. These recordings are what neuroscientists use to measure and analyze neural activity.

Linearity and Time Invariance in the Channel

Showing Linearity and Time Invariance (LTI) is the first step in testing the feasibility of using a linear equalizer to reduce artifact width. Understanding the system-wide ICMS practices not only shows us where we would place the ZFE but also colors our expectation of the linearity through the channel. In our case, the channel is between the output of the current stimulator and the input of the recording DAC. Figure 4 presents an abstracted version of the whole channel in addition to the system-level placement of the ZFE. We choose to place our equalizer on the input-side to simplify our hardware implementation.

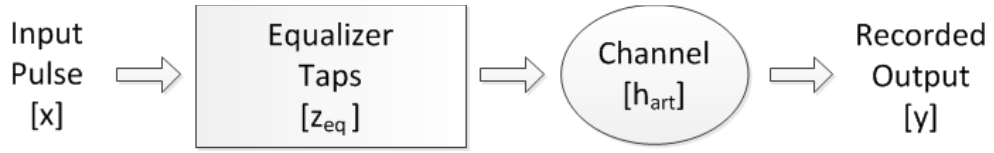

Figure 4: System-Level ICMS Abstraction

This channel has certain nominal hardware limitations on linearity, namely the maximum output compliance voltage of the stimulator and the saturation voltage of the front-end recording amplifiers. These effects can be negated by limiting current amplitudes. The more concerning LTI questions come from the transmission through neural tissue. Without neural tissue being well-studied as an electrical communications channel, we must first define and run tests to determine whether the tissue, and therefore overall channel, can be treated as a Linear Time-Invariant (LTI) system.

Linearity and Time Invariance are generally described with three relationships. Given a relationship from (1), (2) and (4) represent homogeneity and additivity while (3) represents time invariance. To show that the channel is LTI, all three relationships must be confirmed.

$$x_1 \rightarrow y_1 \qquad (1)$$

$$\alpha x_1 \rightarrow \alpha y_1 \qquad (2)$$

$$x_1(t\text{-}T) \rightarrow y_1(\text{t-T}) \quad \text{for all } T \qquad (3)$$

$$x_1(t) + x_2(\text{t}) \rightarrow y_1(t) + y_2(t), \qquad (4)$$

where x_1 and x_2 are arbitrary inputs and y_1 and y_2 are corresponding outputs.

Homogeneity

The relationship between (1) and (2) can be tested by scaling current pulses by $\propto$ and measuring the relative scaling of the output. In particular, the measured scaling factor of the output is calculated with equation (5) where < , > is the inner product and | | is the L^2 norm.

$$\hat{\propto} = \frac{<y_1, y_2>}{|y_1|^2} \quad . \qquad (5)$$

The comparison of $\propto$ to $\hat{\propto}$ indicates the homogeneity of the channel. Using a 10 µA, 250µs current pulse as a baseline, Figure 5 was attained by scaling the current amplitude.

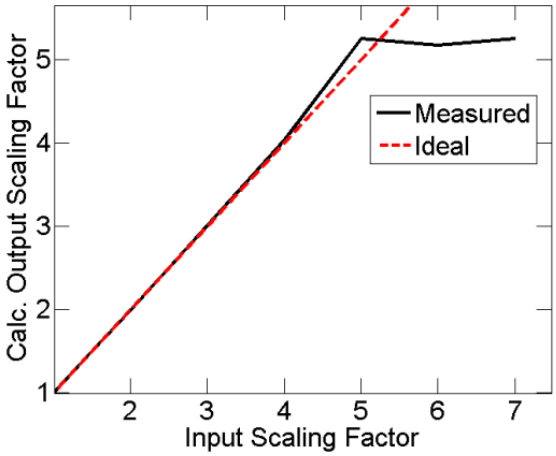

Figure 5: Channel Homogeneity

Figure 5 shows that the channel is homogeneous up to 50µA. Upon closer review, this abrupt saturation occurs not in the neural tissue but rather because of clipping in the Plexon signal acquisition chain. While this does limit the maximum current stimulus to 50µA, the results suggest that the neural tissue itself exhibits homogeneity.

Additivity

To test additivity, the artifacts from 15µA monophasic and biphasic current stimulation were compared. A monophasic waveform is a single current pulse with a given pulse width

and amplitude; a biphasic waveform is a current pulse with a given width and amplitude that is immediately followed by an identical pulse with opposite polarity. Biphasic pulses serve the biological function of maintaining charge neutrality in the neural tissue, but in our case it gives a simple test for additivity. Given the relationship denoted by (5), equation (6) accurately describes the relationship of the biphasic artifact to the monophasic artifact if the channel is additive.

$$input_{biphas}(t) = input_{mon}(t) - input_{mon}(t-T_{pw}) \quad \text{where } T_{pw} \text{ is current pulse width} \qquad (5)$$

$$out_{biphas}(t) = out_{mon}(t) - out_{mon}(t-T_{pw}) . \quad \text{where } T_{pw} \text{ is current pulse width} \qquad (6)$$

The comparison between the ideal biphasic artifact, derived from measured monophasic artifacts and equation (6), and the measured biphasic artifact is seen in Figure 6. While these results are for a 15 µA, 250µs current pulse, similar results exists for various amplitudes and widths.

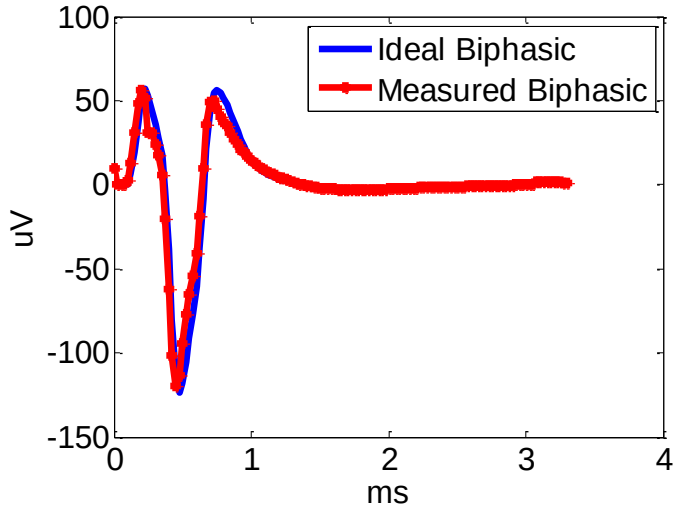

Figure 6: 15µA Ideal Biphasic vs Measured Biphasic Comparison

The measured biphasic response is within 3% of ideal biphasic signal energy. As a result, we conclude that the channel behaves additively and therefore linearly.

Time Invariance

For time invariance, the channel must be consistent for the length of our experiment. As a basic test, we compared various artifacts taken from an 80 second long recording. The individual artifacts and corresponding average artifact seen in Figure 7 are the result of 40μA, 250μs stimuli occurring throughout this 80 second long recording.

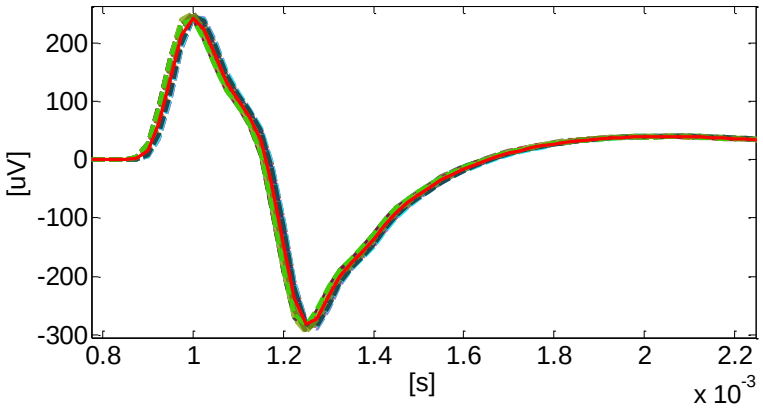

Figure 7: Individual Artifacts (Dotted) vs. Avg. Artifact (Solid Red) from Single Recording

The artifacts match to within 9% of the mean artifact signal energy throughout these recordings despite the presence of underlying neural signals and noise sources. We conclude the overall channel exhibits time-invariance and general LTI behavior.

Reliable Artifact Estimation

Now that the channel is understood and characterized as LTI, we can move forward with the linear equalizer as a valid proposition for reducing the artifact. The focus now turns to finding a robust method to attain a reliable equalizer pattern. The first step of this process is to reliably estimate the channel.

Supply Noise

In all our recordings, there were enormous spikes of signal energy at 60Hz and odd harmonics. Figures 8 and 9 show the time-domain and corresponding frequency spectrum of a 30-second LFP recording in which 20μA, 250μs current pulses were occasionally applied.

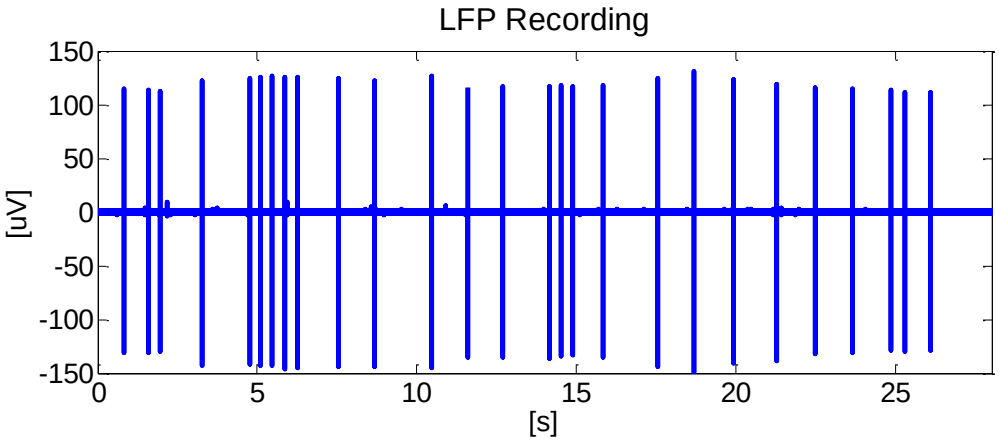

Figure 8: LFP Recording

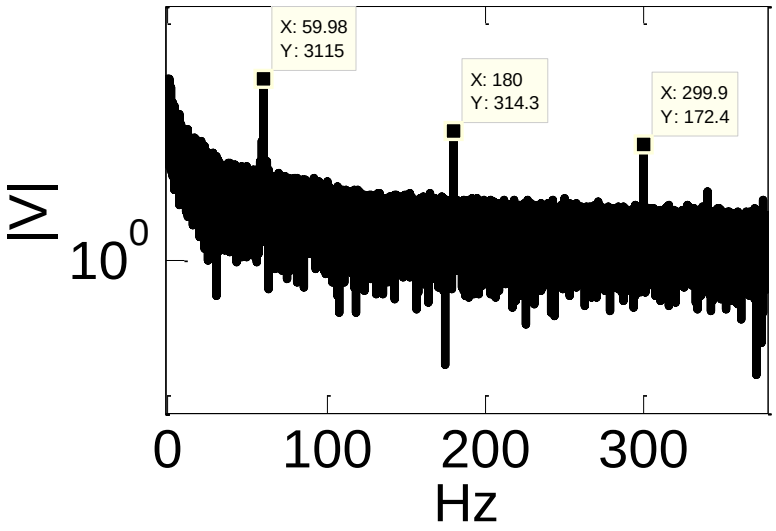

Figure 9: Corresponding LFP Spectrum

The spectrum reveals unnaturally high energies at 60 Hz and odd harmonics, which are regarded as noise from the supplies. The even harmonics do not appear in our recordings because the output is taken differentially. Since these frequencies are so dominated by supply noise, filtering out 60Hz and odd harmonics is the first step in our signal

conditioning chain. Once these frequency spikes are zeroed out in Matlab, the next step is to extract individual artifacts from the overall LFP recording.

Artifact Extraction

The 30 second LFP recording is seen to have artifacts corresponding to the input stimuli. Each spike in Figure 8 is an artifact analogous to that shown in Figure 1. To extract these individual artifacts from the overall recording, we make use of "Event Timing" data, which indicates when stimulation was triggered. However, there can be single sample differences between the actual sample time of the artifact peak versus the sample suggested by the Event Timing. This mismatch occurs due to the discretization of the continuous Event Time that comes with sampling. To correct, we adjust the alignment of individual artifacts around their peak sample time. This method is how the artifacts from Figure 8 were obtained.

Artifact Averaging

To gain a statistically reliable artifact characterization, we average various artifacts from the same recording to come up with our best channel estimate. Assuming that the underlying neural signal can be considered an additive white noise source, averaging helps reduce the electrical noise as the neural noise present in the characterization. Mathematically,

$$y_i = x + w_i \quad \text{has a corresponding SNR of} \quad \frac{|x|}{\sigma_w}$$

$$\text{while} \quad y_{avg} = \frac{\sum y_i}{N} \quad \text{has a corresponding SNR of} \quad \frac{\sqrt{N}|x|}{\sigma_w},$$

assuming that y_i is an individual artifact recording, x is the systematic channel response, w_i are i.i.d noise with variance σ_w, and N is the number of artifacts being averaged.

This averaging effect therefore gives us the most reliable channel estimation. From Figure 7, the red artifact represents the averaged artifact for that LFP recording and the one used for determining an equalizer pattern.

Dead Time

The dead time of the artifact must now be precisely defined. Namely, the exact beginning and end of the artifact must be defined in order to have a meaningful measure for our equalizer. Since the artifact acts as interference to our underlying neural signal, the relative strength of the neural signal to the artifact plays the key role in defining dead time. In our case, the neural signals occurring outside of the artifacts had a measured V_{rms} of 3μV. To be able to see this signal, we constrain that the artifact must be a factor of 10 below this V_{rms} before it is no longer affecting recordings. Accordingly, the beginning and end of the dead time are defined as the first and last time that the artifact was at this level. The definition is seen in Figure 10, which shows the 40μA, 250μs artifact from Figure 1 with bars at this threshold.

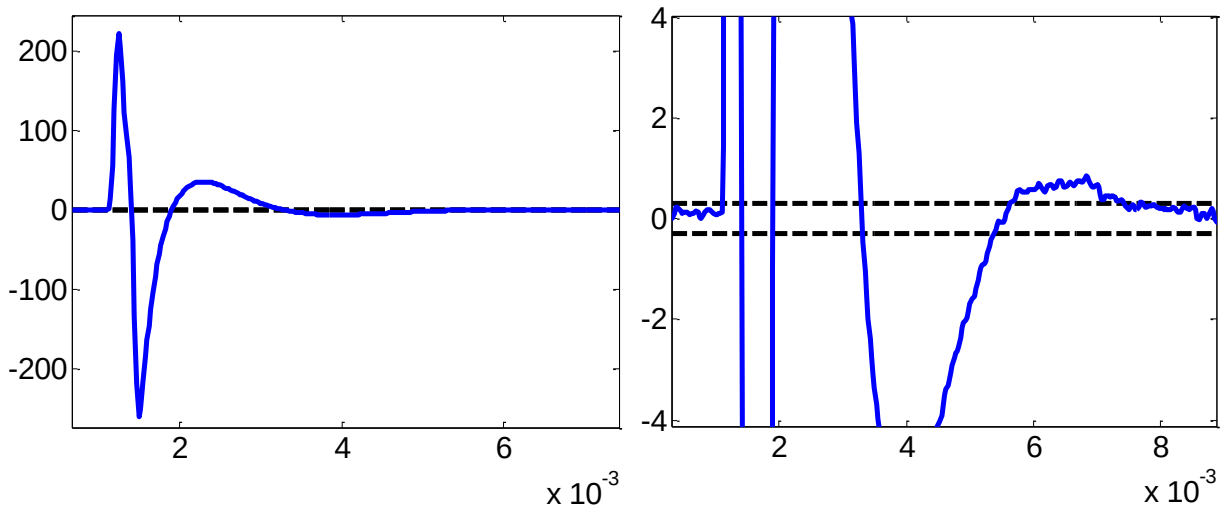

Figure 10: Left, Artifact with Bars; Right, Zoomed In Artifact with Bars

With this definition, the above artifact begins at 1.1ms and ends at 7.9ms, which means the dead-time is 6.8ms.

Linear Equalizer Formulation

With the system assumed to be LTI and now a reliable channel estimate, a linear equalizer can now be formulated to shorten the channel response. Generally, a ZFE attempts to produce an input pulse pattern that will result in a desired output pattern after going through the channel. A first attempt was made with a textbook derivation of the ZFE taps. For ease of understanding, a simple ZFE system diagram is shown in Figure 11. In this figure, the artifact estimate and desired output are included as user-defined inputs and are not part of the equalization path.

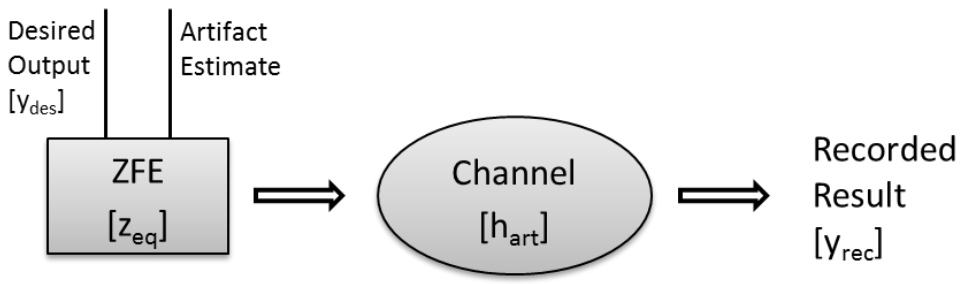

Figure 11: ZFE Visualization

Typical ZFE Derivation

The typical ZFE taps seek to mathematically minimize the Euclidean distance between the output produced by the taps and the desired channel output. Using the visualization of Figure 11, we provide the y_{des} and artifact estimate, and the resulting z_{eq} taps minimize the distance between y_{rec} and y_{des}. The derivation of these taps is shown below, where $\boldsymbol{H}$ is the convolution matrix based on the channel estimation, E is an error measure, $\boldsymbol{y}$ is the vector form of y_{des}, and $\boldsymbol{z}$ is the vector form of z_{eq}.

Minimizing $E = ||\boldsymbol{H}\,\boldsymbol{z} - \boldsymbol{y}||^2$,

$\frac{\partial E}{\partial w_i} = 0 = 2\sum_i H_{ij}\,(\sum_k H_{jk} z_k - y_i)$, or $(\boldsymbol{H}^{\mathrm{T}}\boldsymbol{H})\boldsymbol{z} = \boldsymbol{H}^{\mathrm{T}}\boldsymbol{y}$, which means

$\boldsymbol{z} = (\boldsymbol{H}^{\mathrm{T}}\boldsymbol{H})^{-1}\boldsymbol{H}^{\mathrm{T}}\boldsymbol{y}$.

This derivation gives us a closed form solution for the z_{eq} taps based on desired output and channel estimation. To maintain charge balance, our defined desired output is designed to include the initial upward and downward spikes in the artifact. Figure 12 shows the averaged, unequalized artifact resulting from a 40μA, 250μs current stimulus with our desired output overlaid on top of it.

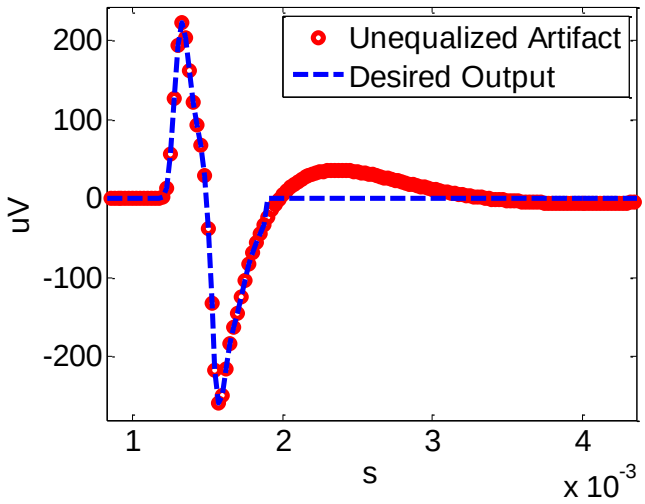

Figure 12: Example of Artifact versus Desired Output

An important step in the equalizer building process is downsampling the artifact once it is well characterized. The current stimulus pulses are 250μs wide while the data is sampled every 25μs, so the original artifact characterization is oversampled by a factor of 10. Thus, the channel characterization must be downsampled in order to get z_{eq} taps that are properly spaced by 250μs. The output of the ZFE is shown in Figure 13, while Figures 14 and 15 compare the unequalized and equalized artifacts.

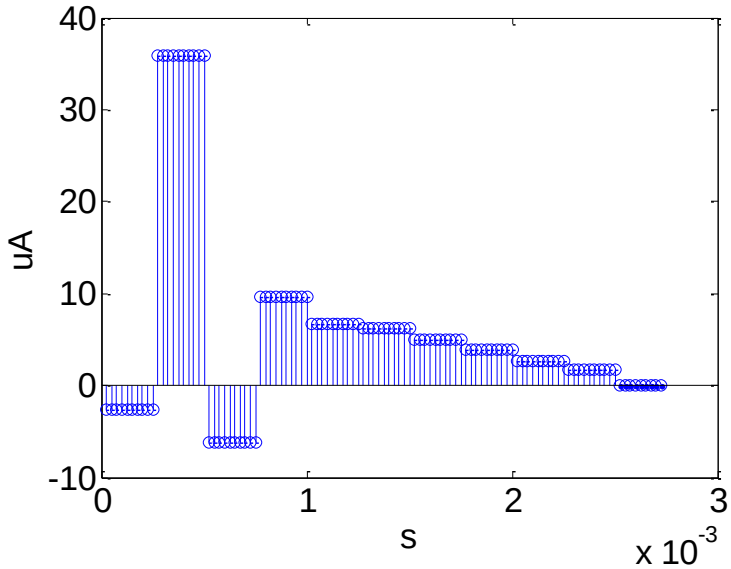

Figure 13: ZFE output

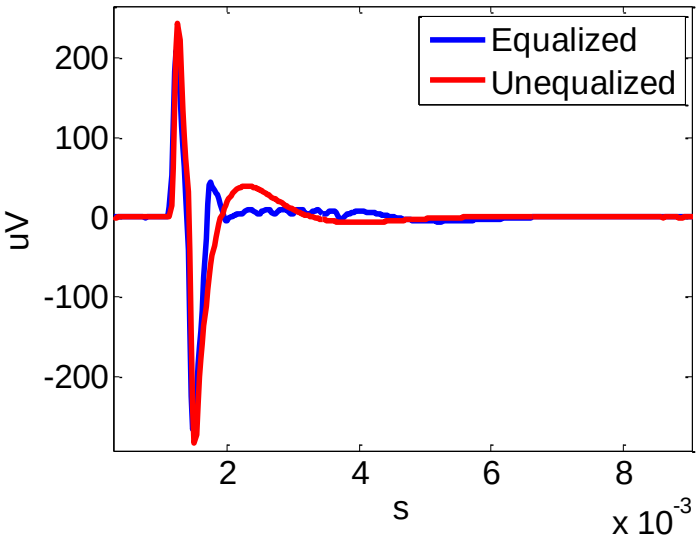

Figure 14: Equalized vs. Unequalized Artifacts

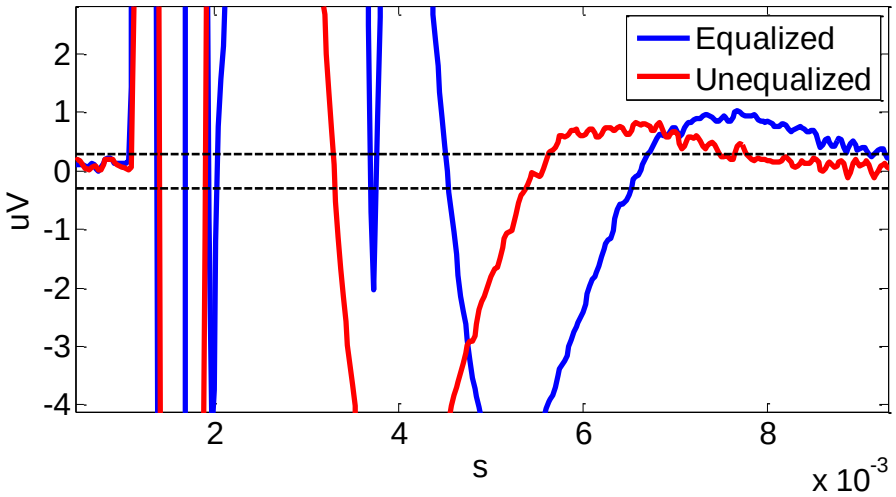

Figure 15: Zoomed-in View with Dead Time Thresholds

There is a significant amount of rippling in the equalized artifact due to the downsampling required to appropriately space the ZFE taps. Compared to the artifact seen in Figure 12, the equalized artifact in Figure 14 still appears to have reduced amplitude after the initial upward and downward spikes. Closer review in Figure 15 shows that while its amplitude appears smaller, the equalized artifact does not go below the threshold set by the V_{rms}

earlier than the unequalized artifact. Thus, dead time is not reduced. As a result, a more computationally complex but robust equalization algorithm was explored.

Channel Inversion Algorithm

Since the previous linear attempt proved to be insufficient, we proceeded with a channel inversion algorithm that is more computationally intense but also more robust. The present implementation has all the computation done in Matlab, so the added complexity is a negligible cost. At a high level, this algorithm finds a transfer function that best fits the measured channel response and then produces an impulse response that stably inverts this transfer function and produces our desired output pattern.

Again, the averaged artifact is first downsampled by 10 to again make the 250μs wide pulse appear as a Kronecker Delta. This downsampled artifact is then treated as a channel impulse response. The Steigtlitz-McBride algorithm for an autoregressive-moving-average (ARMA) model fits this impulse response to an s-domain transfer function with numerator and denominator of degree N. In our case, we found that using a degree of 4 produced an inverse response that was not under or over-damped. Next, we obtain our ZFE's transfer function by taking the inverse of this transfer function, eliminating the unstable poles, and then multiplying by the Laplace transform of our desired channel output. The last step is included so the output of the overall system is near our desired output. This finalized s-domain function is then mapped back to the time-domain to produce an impulse response for our ZFE. This process, run for the 40μA, 250μs artifact, is summarized in the following Figures.

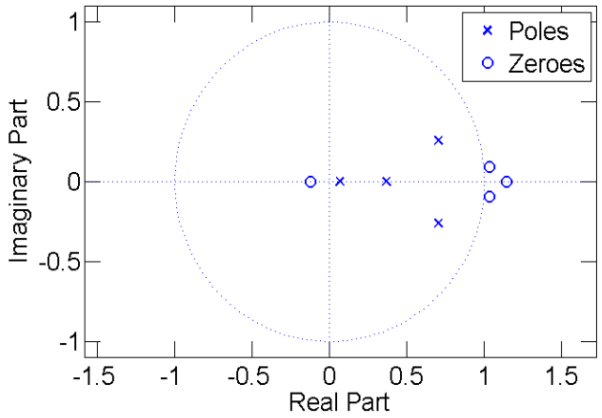

Figure 16: Pole-Zero Plot of Fitted Channel Transfer Function

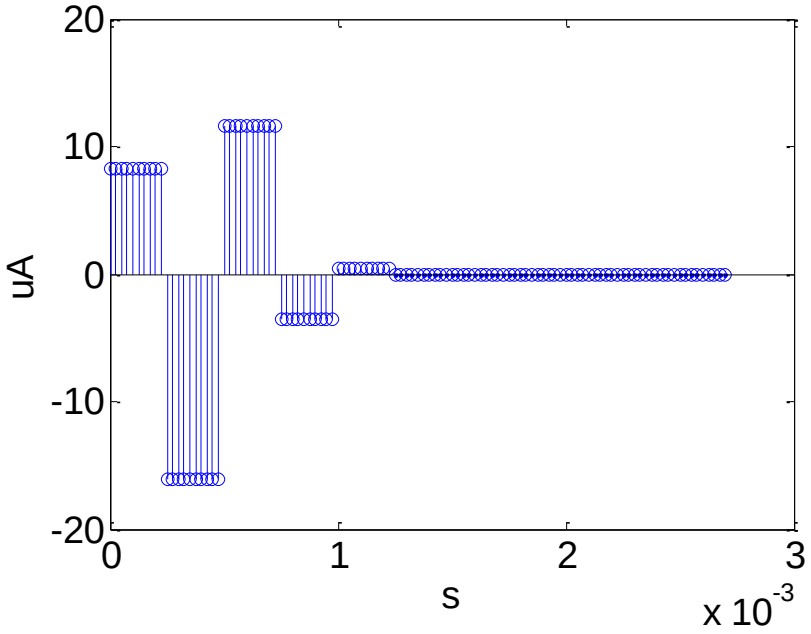

Figure 17: ZFE Output

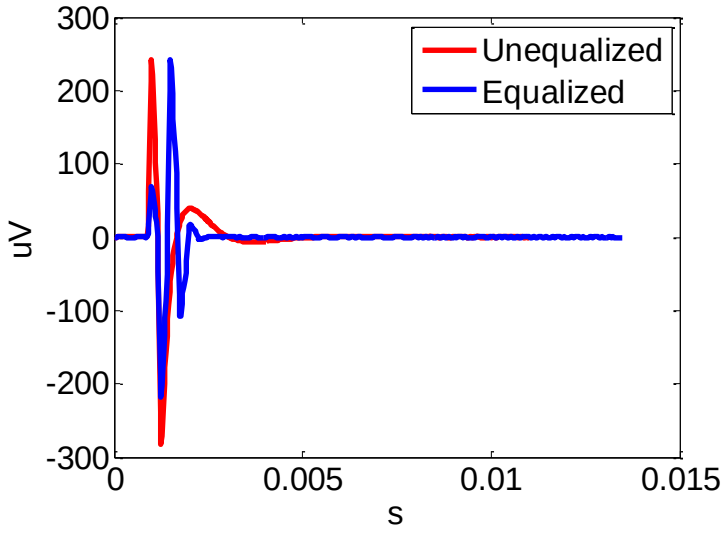

Figure 18: Equalized vs. Unequalized Artifacts

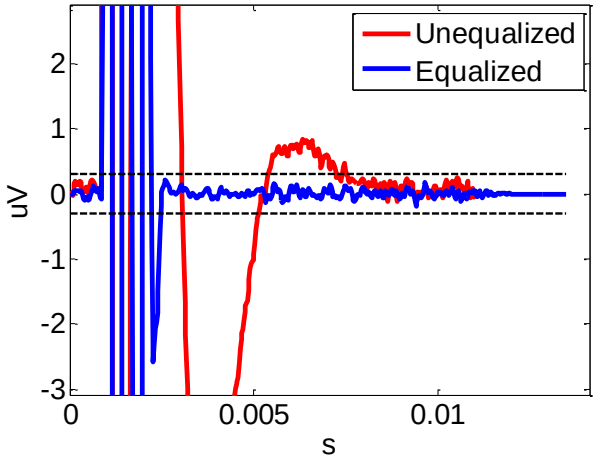

Figure 19: Zoomed-in View with Dead Time Thresholds

From Figure 19, the dead time has been reduced from 6.8ms to 1.8ms, a reduction of 73%. This formulation of the equalizer proves robust enough to quiet the equalized artifact well below our floor for dead time. While the channel inversion is imperfect due to the removal of unstable poles, the algorithm is sufficient for significantly reducing the width of the averaged artifact.

Up to this point, our equalizers have been run on the averaged data. For the sake of completeness, we must now ensure that our ZFE pattern works for individual artifacts on individual channels.

Equalizing Individual Artifacts

We first ensure that the equalizer is effective for non-averaged artifacts from the same channel. In other words, this test confirms that the ZFE pattern will be effect for individual artifacts, not just the averaged artifact. Several equalized artifacts from a single channel are shown in Figure 20. While there is a small amount of variance, the overall reduction in dead time shows that the equalizer is well suited for the individual artifacts from a single channel. All figures in this section are from stimulations with 40μA, 250μs current pulses.

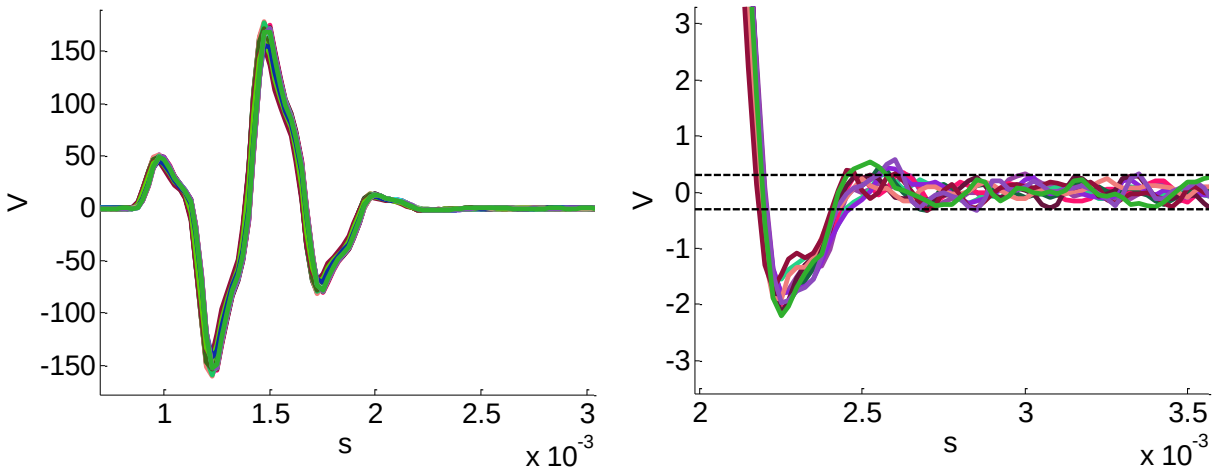

Figure 20: Left: Equalized Artifacts, Right: Artifacts with Dead Time Thresholds

Since one stimulating electrode interacts with many different recording electrodes, we next confirm that a single ZFE pulse pattern from the stimulating electrode will suffice for the many recording electrodes. Given the highly coupled nature of these channels, we expect the equalizer to indeed work across the channels. Figure 21 shows the overlaid equalized

artifacts for each of the 6 active recording sites, and Figure 22 displays the reduction in dead time across these 6 channels.

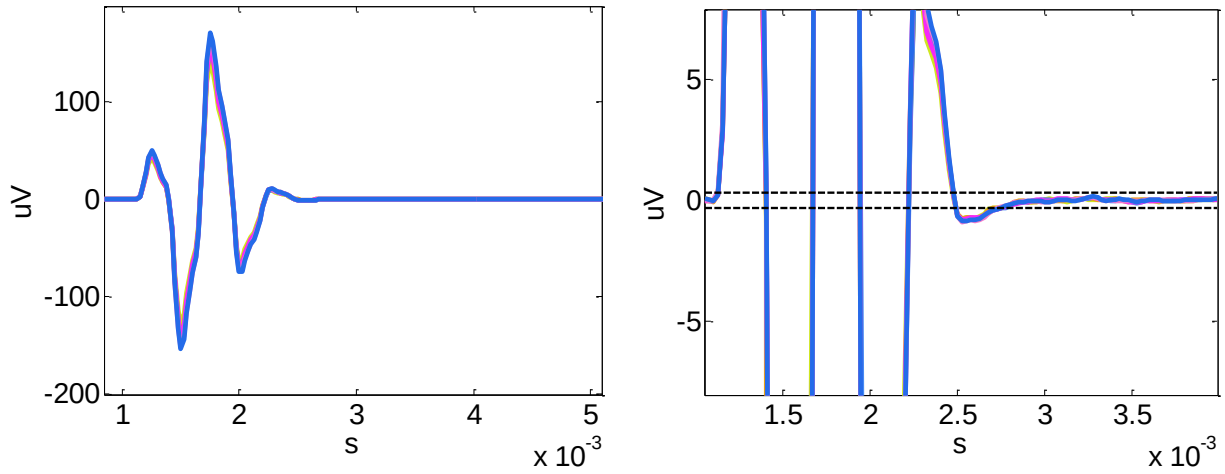

Figure 21: Left, Equalized Artifacts; Right: Zoomed-In View with Dead Time Thresholds

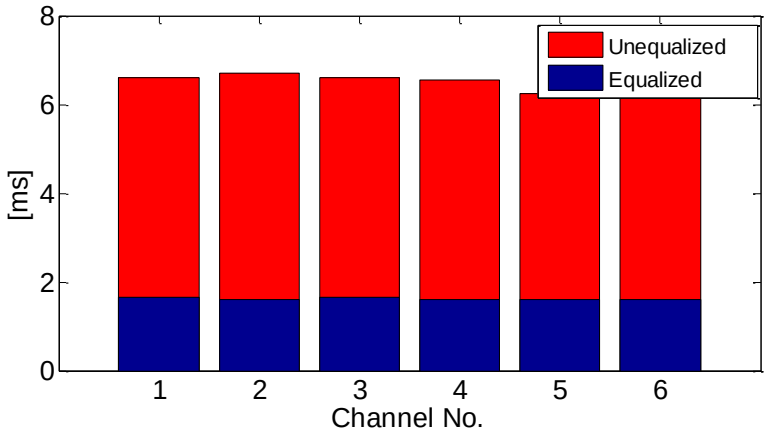

Figure 22: Dead Time Reduction vs. Channel

The equalizer indeed proves to be effective across the individual channels. Now that we have confirmed that the equalizer can be used for individual artifacts across parallel channels, we look next to building hardware requirements for implementing this filter in a real ICMS experiment.

Equalizer Hardware Considerations

The system-level architecture of the equalizer is shown in Figure 23. The ZFE algorithm provides tap weights, and a Digital-to-Analog Converter (DAC) turns these tap weights into current pulses. For our equalizer, the DAC will have a current output, and relevant specifications for the hardware chain are number of equalization taps, DAC full-scale current, DAC current resolution, and output compliance voltage.

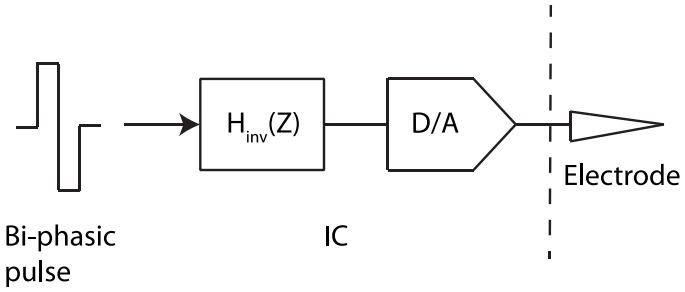

Figure 23: System-Level Design of the Equalizer

Since the homogeneity of the channel saturates at 50μA, we chose to design towards equalizing a 40μA current stimulus. The following work is therefore based on the artifacts produced by a 40μA, 250μs current pulse.

Number of Taps

The number of taps on the equalizer has implications towards hardware complexity and power consumption. Since the end goal is to have an implantable equalizer device, we would like to drive the power consumption as low as possible. Thus, the optimal design has the minimum number of equalizer taps. To analyze this, we sweep the number of taps and find corresponding dead time. From the Figure 24, the minimum number of taps required to obtain full dead time reduction is 5 taps. To be safe, we design for 6 taps.

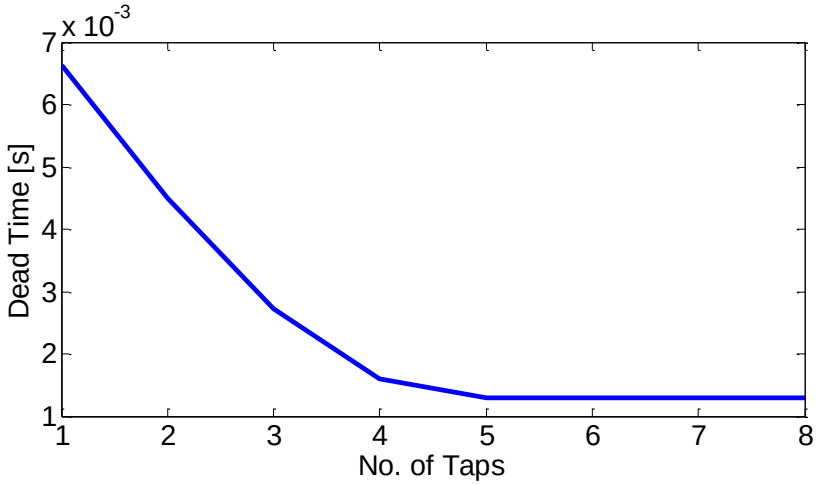

Figure 24: Dead Time vs. Number of Taps

DAC Specifications

While our current design focuses on equalizing a 40μA pulse, we would like to increase the full scale current to the upper limits of typical ICMS ranges. If recording equipment is improved and the channel no longer saturates, having a higher full scale current will provide more flexibility. The target full scale current is thus set at 100μA, which is at the higher end for ICMS [1].

Considering the equalization for a 40μA stimulus, we must ensure that the DAC has sufficient current resolution. Sweeping the number of bits in the DAC provides a relationship between the number of bits and the dead time reduction. This relationship, derived in Matlab and seen in Figure 25, shows us that for a DAC with 100μA full scale current, 12 bits of resolution are required to reduce dead time for the 40μA equalization pattern.

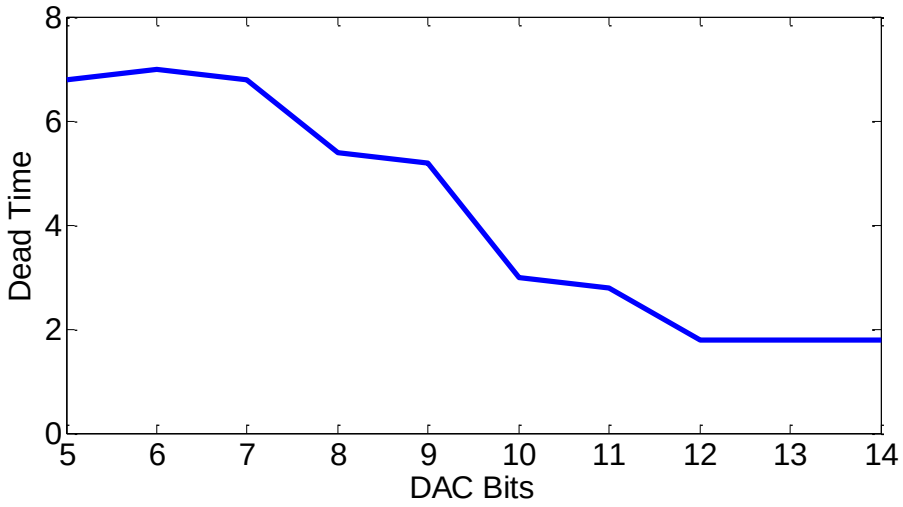

Figure 25: DAC Bits vs. Dead Time

Output Compliance Voltage

The final major factor in the hardware chain is the output compliance voltage. Given the importance of maintaining linearity in the system, the voltage must be high enough to prevent clipping. However, an arbitrarily high compliance voltage makes an implanted equalization system impractical. Our current pulses will see a maximum output impedance of approximately 100kOhms. With a full-scale current of 100μA, the minimum output compliance voltage is therefore 10V.

Figure 26 summarizes the hardware requirements.

No. Of Taps	6
DAC Full-Scale Current	100μA
No. of DAC Bits	12
Output Comp. Voltage	10V

Figure 26: Hardware Specifications

Conclusion

Current work focuses on building the hardware to test in a real animal experiment. Given the various hardware requirements, the solution has proved illusive. Building the system out of discrete components on a PCB is highly constrained by the current precision and compliance voltage, while solutions from industry lack the full programmability necessary to create the equalizer pattern. Once this problem is solved, we will be able to fully test the equalizer in a real ICMS experiment.

Overall, the application of equalization to microstimulation has shown promise in shortening the length of the ICMS artifact and allowing recovery of the underlying signal. With hardware implementation as the focus of ongoing work, we have built a strong theoretical framework that is growing towards the end goal of testing in a live environment.

Acknowledgements

First and foremost, I would like to thank Rikky Muller and Jan Rabaey for entrusting me with this project as an undergraduate. Rikky, your mentorship during the past few years has been my most valuable learning resource. I'd also like to thank Aaron Koralek for always making time for me in the animal laboratories and Simone Gambini for propelling this project forward. Lastly, I'd like to thank my family and friends for always buoying me through the down times and celebrating during the good.

References

[1] M.R. Cohen, W.T. Newsome. "What electrical microstimulation has revelead about the neural basis of cognition." Science Direct. Vol. 14, No. 2, Apr. 2004.

[2] D.R. Merrill, M. Bikson, J.G.R. Jefferys. "Electrical stimulation of excitable tissue: design of efficacious and safe protocols." J. of Neuroscience Methods. Vol. 141, 2005.

[3] A. Jackson, J. Mavoori, E.E. Fetz. "Long-term motor cortex plasticity induced by an electronic neural implant." Nature, vol. 444, pp. 57-60, Nov. 2006.

[4] L. Szczecinski. "Low-Complexity Search for Optimal Delay in Linear FIR ZFE Equalization." IEEE Signal Proc. Letters. Vol. 12, No. 8. Aug.

[5] S. Venkatraman, J.D. Long, K. Elkabanny, Y. Yao, J. Carmena. A system for neural recording and closed-loop intra-cortical microstimulation in live, awake rodents, IEEE Trans. on Biomedical Eng, 56(1), pp. 15-22, Jan. 2009.

[6] D. Wagenaar, S. Potter. "Real-time multi-channel stimulus artifact suppression by local curve fitting." J. of Neuroscience Methods, vol. 120, pp.113-120, May 2002.

[7] L. Rossi, G. Foffani, S. Marceglia, F. Bracchi, S. Barbieri, A. Priori. "An electronic device for artefact suppression during deep brain stimulation." J. of Neural Eng., Apr. 2007

[8] S. Stanslaski, P. Afshar et. Al. Design and Validation of a Fully Implantable, Chronic, Closed-Loop Neuromodulation Device with concurrent sensing and stimulation IEEE Trans. on Neural System and Rehabilitation Eng., July 2012

[9] E.G. Jones, "Rattus Norvegicus" Dataset r3778, http://brainmaps.org.

[10] K. Steiglitz, and L.E. McBride, "A Technique for the Identification of Linear Systems." IEEE Trans. Automatic Control, Vol. AC-10, pp. 461-464. 196

[11] Plexon User Manual